*Journal of Structural Geology*, Vol. 15, No. 11, pp. 1303 to 1313, 1993
Printed in Great Britain

0191-8141/93 $06.00+0.00


# Rotation of biotite porphyroblasts in pelitic schist from the Nukata area, central Japan

AKIRA MIYAKE

Department of Earth Sciences, Aichi University of Education, Kariya 448, Japan

(*Received* 6 *May* 1992; *accepted in revised form* 2 *November* 1992)

**Abstract**—The detailed microstructures of biotite porphyroblasts in pelitic schist from the Nukata area, central Japan, indicate that the porphyroblasts rotated in an external reference frame during non-coaxial deformation. The amount of rotation and rotation axis are controlled by the (001) orientation of the biotite porphyroblast with respect to the schistosity and the lineation. Concurrently with rotation, the biotite porphyroblasts suffered shape change by solution and deposition in the shortening and dilating fields around the porphyroblast, respectively. The close co-occurrence of inclusion-free domains (newly deposited biotite domains) and pressure shadows along the (001) faces suggests that continuously opening fractures along the (001) faces caused biotite deposition as well as pressure shadow aggregates. The role of pressure shadow formation for porphyroblast rotation is discussed in terms of stresses applied on the porphyroblast surface. It is concluded that although the formation of 'deformation-partitioning-induced pressure shadows' tends to suppress porphyroblast rotation, that of 'fracture-induced pressure shadows' ('pressure fringes') promotes porphyroblast rotation. The present biotite porphyroblasts would have rotated at rates depending not only on their shape and shape orientation, but also on the (001) orientation.

## INTRODUCTION

INCLUSION trials in porphyroblasts are important since they give information about matrix fabrics present during porphyroblast growth. They have been used in estimating the time relation of deformation and crystallization during metamorphism (e.g. Zwart 1962, Spry 1963, Rast 1965).

Inclusion trials (*Si*) in pre- or syn-kinematic blasts, which may be straight, sigmoidal or spiralling, are commonly discordant to surrounding foliations (*Se*). The discordance has generally been interpreted as being due to rotation of porphyroblasts during deformation (e.g. Cox 1969, Powell & Treagus 1970, Williams & Schoneveld 1981, Olesen 1982, Lister & Williams 1983, Lister *et al.* 1986, Passchier *et al.* 1992). However, Ramsay (1962) showed that coaxial flattening oblique to the foliation can produce a similar discordant relationship between *Si* and *Se* without porphyroblast rotation. Accordingly, Bell (1985) discussed the proposal that porphyroblasts generally do not rotate with respect to external geographic co-ordinates, even during non-coaxial bulk deformation, because porphyroblasts are usually positioned in progressive shortening zones of the strain-field diagram of Bell (1981) as a result of deformation partitioning. Fyson (1975, 1980), Steinhardt (1989), Bell & Johnson (1989), Johnson (1990) and Hayward (1990, 1992) demonstrated that *Si* orientation is almost constant throughout wide areas where intense deformation continued after porphyroblast growth and concluded that the discordant relationship between *Si* and *Se* is due primarily to rotation of *Se*.

On the other hand, if the assumption that rocks deform like slowly flowing fluids is valid, it is expected that rigid porphyroblasts in deforming rocks should generally rotate by significant amounts. When the deformation is Newtonian, rotational behavior of isolated ellipsoidal porphyroblasts can be modeled using Jeffery's (1922) theory (e.g. Gay 1968, Ghosh & Ramberg 1976, Passchier 1987). It is possible that real rock deformation is not Newtonian but follows a power law (e.g. Carter 1976). However the implications for rotational behavior of the two deformation laws is probably similar (Ferguson 1979).

When porphyroblasts rotate during ductile deformation, the rotation rate and rotational axis depend on their shape and orientation with respect to the strain field (e.g. Passchier 1987) and so it is expected that non-equidimensional porphyroblasts in different initial orientation may rotate about different axes by different amounts. For example, Zwart & Calon (1977) reported that the lath-shaped chloritoid porphyroblasts from Curaglia, in the Swiss Alps, had rotated in different directions during flattening deformation orthogonal to the foliation, according to whether their initial long axes lie in clockwise or anticlockwise direction from the foliation.

Seo & Hara (1980) reported that discordant angles between *Se* and *Si* in biotite porphyroblasts vary systematically according to the angle between *Se* and the (001) plane of biotite porphyroblasts in the Ryoke metamorphic schists from the Nukata area, central Japan. They did not regard this evidence as a result of rigid body rotation of biotite porphyroblasts.

This paper describes biotite porphyroblasts in pelitic schist from the same area as treated by Seo & Hara (1980). Detailed observations indicate that the biotite porphyroblasts in the schist did rotate in an external reference frame. Vernon (1988) reported that clear evidence of rotation of biotite porphyroblasts is uncommon in the literature. This investigation gives new evidence of such rotation.

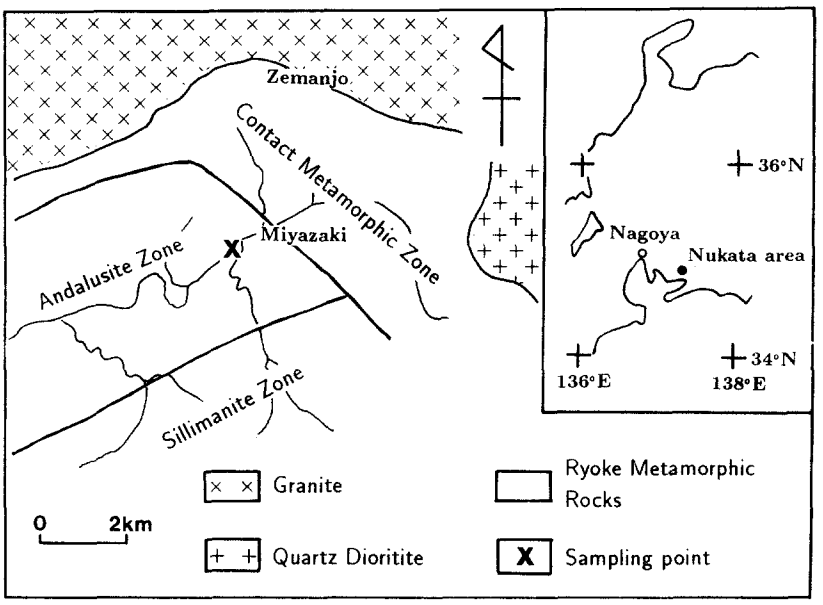


Fig. 1. Geological sketch map with the locality of the Nukata area.

## GEOLOGICAL SETTING

The Ryoke metamorphic rocks of the Nukata area consist mainly of pelitic and psammitic schists, and metachert. Kano (1978) related these meta-sedimentary rocks to the Triassic system in the non- or weakly metamorphosed area. The metamorphic age of the Ryoke belt is inferred by K–Ar and Rb–Sr methods to be in the range of 60–90 Ma (e.g. Nozawa 1977). The metamorphic rocks of the area were intruded by granitic rocks in the northern and eastern parts during late- or post-regional metamorphism.

Figure 1 shows the metamorphic zoning in the area. The metamorphic grade ranges from andalusite grade in the northern part to sillimanite grade in the southern part (Asami & Hoshino 1980, Asami *et al.* 1982, Seo 1985) although a contact metamorphic zone is developed around the granitic bodies (Asami & Hoshino 1980, Seo 1985). $Al_2SiO_5$ mineral-bearing rocks usually contain K-feldspar in the sillimanite and contact metamorphic zone, but not in the andalusite zone. The contact metamorphic zone is characterized by the widespread mineral assemblage cordierite + K-feldspar in pelitic and psammitic rocks.

The schistosity of metamorphic rocks in the area is generally parallel to the original bedding and has a consistent ENE–WSW trend with monotonous dips of 20–80°N. The orientation of mineral lineations is also consistent throughout the area and has a gentle pitch toward ENE or WSW. Mesoscopic folds are scarce.

The deformation history in the area was discussed by Seo & Hara (1980). They divided the deformation history after porphyroblastic growth of biotite into two stages: a first stage of intracrystalline slip of biotite and a subsequent stage of pressure solution deformation. I will challenge this interpretation in the present paper.

## SAMPLE DESCRIPTION

The studied pelitic schist was collected in the andalusite zone about 200 m west of Miyazaki (Fig. 1). The sample shows homogeneously developed unfolded schistosity, which is parallel to the bedding plane, and a weak mineral lineation which can be recognized on the schistosity planes.

The schist is composed predominantly of quartz, muscovite and biotite. Biotite crystals usually occur as elongate porphyroblasts ranging from 0.1 to 1 mm in their longest dimension. The matrix consists of equal amounts of lath-shaped muscovite and elongate quartz grains. Minor amounts of fine-grained graphite also occur ubiquitously in the porphyroblast and matrix minerals, and also along grain boundaries of matrix minerals. The schist is homogeneous on the scale of the thin section, except for the presence of a weak compositional layering and for quartz veins that are usually parallel to the schistosity. Muscovite grains with an average size of 0.005 × 0.05 × 0.1 mm have strong preferred lattice and dimensional orientations. The schistosity and the mineral lineation are defined by this arrangement of muscovite flakes. Biotite and elongate quartz crystals also show preferred dimensional orientation, which is consistent with the schistosity.

## MICROSTRUCTURE OF BIOTITE PORPHYROBLASTS

Detailed observations were made using three thin sections (Fig. 2): one perpendicular to the lineation (**a**-section), one perpendicular to the schistosity and parallel to the lineation (**b**-section), and one parallel to the schistosity (**c**-section).

Although muscovite flakes show strong preferred lattice orientation, the lattice fabric for biotite is weak

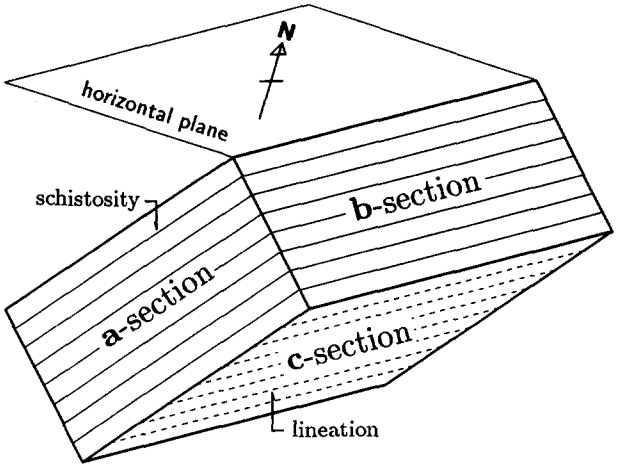


Fig. 2. Schematic block diagram defining the a-, b- and c-sections.

(Fig. 3). Because of this weak lattice fabric, biotite porphyroblasts with various orientations with respect to the schistosity and the lineation can be observed in the sample.

Several characteristics of biotite porphyroblasts vary according to their (001) orientation. The variations were mainly observed in the **a**- and **b**-sections. In these thin sections, the characteristics vary remarkably in the porphyroblasts with (001) at high angles (more than 60°) to the thin section planes (referred to below as 'upright biotite'). Thus, variation patterns in the angle between the (001) trace and the schistosity trace (referred below as 'inclination angle') will be described for 'upright biotite'. For these 'upright biotites', the observed 'inclination angle' in two-dimensional section will be close to the true three-dimensional angle between (001) and the schistosity. The convention used here is that the 'inclination angle' is taken as positive when the orientation is inclined from the schistosity in the anticlockwise direction looking down for the **b**-section and to the north for the **a**-section. In order to construct the full three-dimensional image, biotite porphyroblasts with (001) at low angles (less then 30°) to the thin section (referred to below as 'recumbent biotite') will be also described.

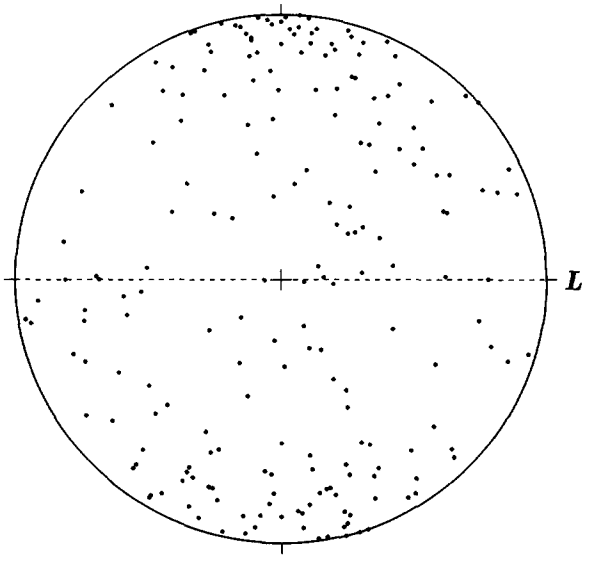


Fig. 3. Scatter diagram for (001) poles of biotite grains. Plotted orientations are measured in the **b**-section. A dashed line and the symbol 'L' represent schistosity and lineation, respectively. The diagram shows a weak lattice fabric with monoclinic symmetry.

*Shape, elongation orientation and axial ratio*

'Upright' and 'recumbent biotites' in the **a**- and **b**-sections usually have a lenticular shape (Figs. 4a–f and 5), although their elongation orientation and axial ratio vary according to the (001) orientation as described below. On the other hand, 'upright biotites' in the **c**-section have a rectangular shape elongated along the (001) trace, regardless of the orientation of the (001) trace (Figs. 4g & h).

Elongation orientations were measured as the orientations of the longest axis and axial ratios were obtained by calculating $l_1/l_2$, where $l_1$ is the longest intercept length and $l_2$ is the intercept length in the direction 90° away from the longest axis.

Figures 6(a) & (b) show the relationship between the elongation orientation and the axial ratio in the **a**- and **b**-sections, respectively. The elongation orientation tends to be parallel to the schistosity for biotites with high axial ratios in both **a**- and **b**-sections. However, this tendency is weaker for lower axial ratios. The departure of the elongation orientation from the schistosity trace for lower axial ratios is larger in the **a**-section than in the **b**-section. Such a dimensional fabric of biotite is consistent with the orientations of the schistosity and the lineation.

Figures 7 and 8 are plots of elongation orientations and the axial ratios against the 'inclination angle' for 'upright biotites' in **a**- and **b**-sections. Both elongation orientations and axial ratios are controlled mainly by the (001) orientation. With increasing 'inclination angle', the angle between the elongation direction and the schistosity trace increases and the axial ratio decreases in both the **a**- and **b**-sections.

*Inclusion trails*

Each biotite porphyroblast could be divided into two kinds of domains; the first domain contains many inclusions of fine graphite and minor amounts of quartz, and the second domain contains no or scarce inclusions. The boundary of the two domains is usually sharp (Figs. 4 and 5).

The inclusions show essentially straight arrays for the 'upright' and 'recumbent biotites' in both **a**- and **b**-sections (Figs. 4a–f and 5) while most biotite grains in the **c**-section contain an isotropic inclusion pattern (Figs. 4g & h) due to low angle intersection of *Si* planes. In many cases *Si* is not continuously linked to *Se* but truncated by *Se* or separated from *Se* by the inclusion-free domain.

*Si* orientations were measured as discordance angles relative to the *Se* traces in the **a**- and **b**-sections. The *Si* orientation systematically varies according to the (001) orientation. Figures 9(a) & (b) show the variation

patterns of the *Si* orientation of 'upright biotites' against the 'inclination angle' for the **a**- and **b**-sections, respectively. The variation pattern for the **a**-section is symmetric with respect to the *Se* orientation while that for the **b**-section is asymmetric. On the other hand (001) traces of 'recumbent biotites' are always sub-parallel to the *Se* trace (Fig. 5h).

*Inclusion-free domains*

Inclusion-free domains usually occur parallel to the (001) face at both ends of the biotite grain (Figs. 4 and 5). The shape of the domain shows monoclinic symmetry with respect to the center of the grain. The inclusion-free domain sometimes has a characteristic hook-like tail at one end corner of the (001) face (Figs. 4d & e and 5b & c). This inclusion-free domain is usually accompanied at its outside by pressure shadow aggregates and is comparable with the 'paired clear zone' of Lister *et al.* (1986).

*Pressure shadows*

Pressure shadows are composed of inclusion-free aggregates of quartz and minor amounts of lath-shaped muscovite. The quartz grains in well-developed pressure shadows are usually elongated along the direction perpendicular to the (001) face (Figs. 4g & h). The degree of pressure shadow development is also controlled mainly by the (001) orientation. Roughly speaking, when the (001) plane lies at high angles to the schistosity, especially to the lineation, biotite tends to have large pressure shadows (cf. Mancktelow 1979). However, detailed observation indicates that, for the **b**-section, upright biotite grains with a positive 'inclination angle' tend to have a larger pressure shadow compared to those with a negative 'inclination angle' (for example compare Figs. 5e & f). On the other hand, the upright biotite in the **a**-section has similarly sized pressure shadows for positive and negative 'inclination angles' of the same magnitude.

## INTERPRETATION

*Shape change of biotite porphyroblasts*

The weak lattice fabric (Fig. 3) of biotite grains suggests that the biotite porphyroblasts nucleated and grew under relatively static conditions (see also Seo & Hara 1980). Such conditions are incongruous with the strong preferred lattice and dimensional orientation of muscovite flakes which defined the schistosity and the lineation. On the other hand, the dimensional fabric (Fig. 6) of biotite is congruous with the muscovite fabric. From these observations, it is considered that biotite porphyroblasts grew and enclosed an earlier schistosity during an interkinematic stage, and that subsequently biotite grains suffered shape change during development of the existing schistosity.

The *Si* traces in the biotite porphyroblasts in the **a**- and **b**-sections are usually truncated at the interfaces sub-parallel to the schistosity by the *Se* traces. This suggests that local mass removal of biotite components took place at these interfaces. On the other hand, new biotite material would have grown as inclusion-free domains in dilating pressure shadows. The growth has occurred from the (001) face of the old grain, which remains as an inclusion-crowded domain. The development of pressure shadows and the inclusion-free domains are most advanced when the (001) faces are at high angles to the schistosity, and especially to the lineation.

The pressure shadows can be interpreted as sites where minerals deposited in an opening fracture around a rigid porphyroblast during matrix deformation (Lister *et al.* 1986). The mica (001) face would have been a suitable face for fracturing since its surface energy is characteristically low. Thus when the (001) face is at a high angle to the extension direction of the matrix deformation, a pressure shadow will be developed to a larger degree. This suggests that the lineation orientation is approximately parallel to the principal maximum extension axis and that the intermediate axis, which is approximately parallel to the schistosity and perpendicular to the lineation, is also extended.

Solution in the shortening fields around a porphyroblast and deposition in the extending fields could lead to shape change of biotite grains such that their elongation orientation would tend to be parallel to the schistosity (cf. Beutner 1978) as shown in Fig. 6. The nature of such a shape change should vary according to the initial elongation orientation, which is related to the (001) orientation, as shown in Figs. 7 and 8.

*Rotation of biotite porphyroblasts*

The discordance between *Si* and *Se* can be interpreted geometrically in several ways: (1) *Se* rotation without porphyroblast rotation; (2) *Si* rotation by intracrystalline slip on (001) without rotation of the (001) orientation; (3) rigid body rotation of the biotite grains with or without intracrystalline slip on (001).

The first interpretation above is rejected since it is difficult to explain the systematic variation of the *Si* orientation with respect to the (001) orientation (Fig. 9). The systematic *Si* variation suggests that the *Si* planes have rotated with respect to each other.

The second interpretation was proposed by Seo & Hara (1980), who also studied biotite porphyroblasts from the present area. They reported a similar variation pattern to that of Fig. 9(a) in **a**-sections. They concluded that *Si* of biotite flakes rotated in the opposite direction to (001) due to intracrystalline slip along the fixed (001) plane during a progressive compression in a direction parallel to the schistosity trace in the thin section. Although their interpretation can explain the systematic variation of the *Si* orientation, it is not reasonable since such intracrystalline deformation will in general also be accompanied by rotation of the (001) orientation (e.g. Etchecopar 1977).

Thus the third interpretation remains. In this interpre-

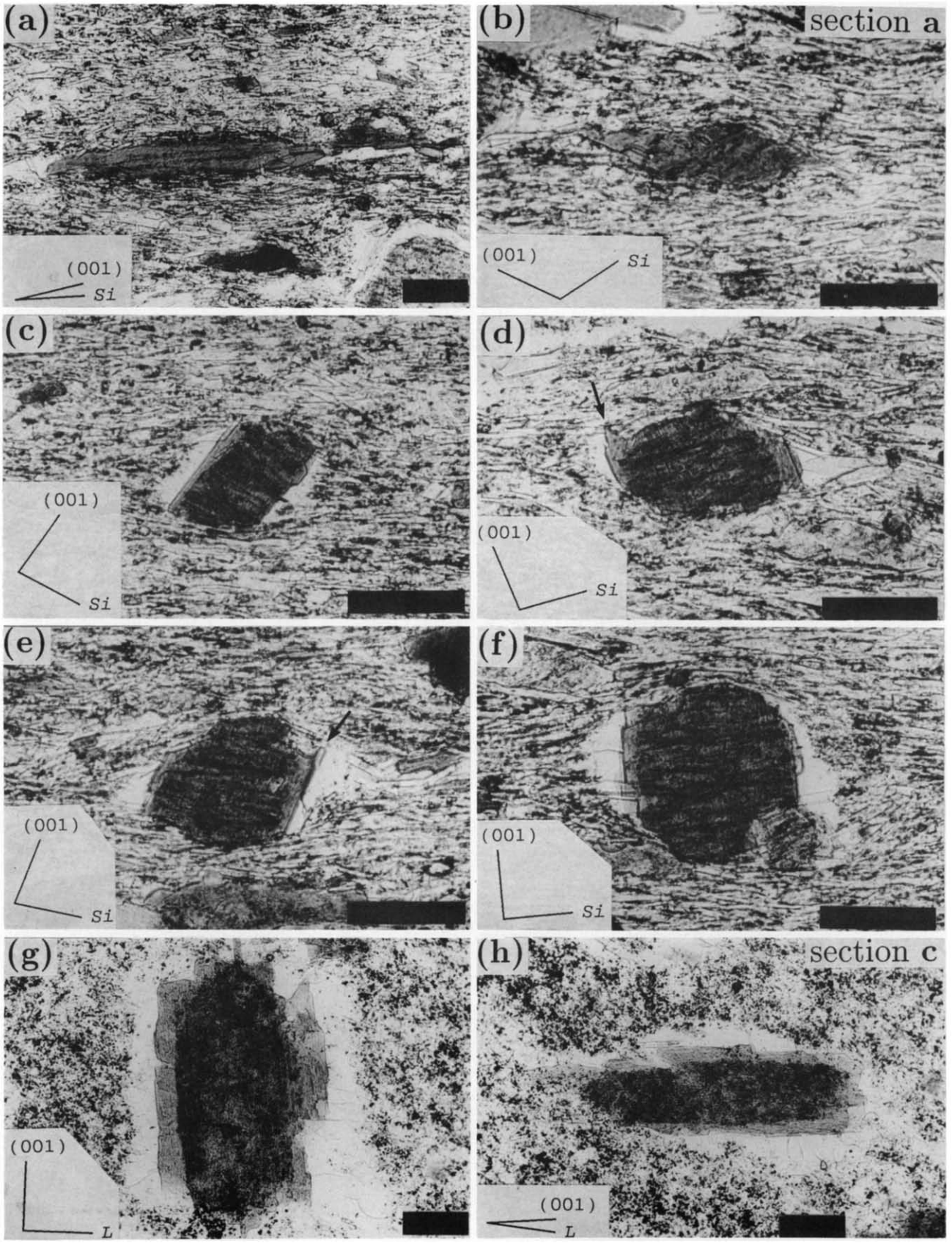


Fig. 4. (a)–(f) 'Upright biotites' with various 'inclination angles' in the **a**-section. *Si* is sub-parallel to *Se* in biotites with (001) at low (a) and high (f) angles with *Se* while biotites with intermediately inclined (001) show inclined *Si* (b, c, d & e). Pressure shadows develop to a large extent when (001) is at high angle with *Se* (f). When (001) or *Si* are inclined at intermediate angles, inclusion-free domains around porphyroblasts occasionally have hook-like tails (arrows in d and e). (g) & (h) 'Upright biotites' with the (001) plane at a high angle to the lineation (g) and at a small angle with the lineation (h) in the **c**-section. Intersection outline shape of these biotites and inclusion-crowded domains show rectangular shape elongated along (001). Quartz and muscovite in the pressure shadows are elongated along the direction at high angles with the (001) faces. Pressure shadows and inclusion free domains in (g) are larger than in (h). Scale bars are 0.1 mm.

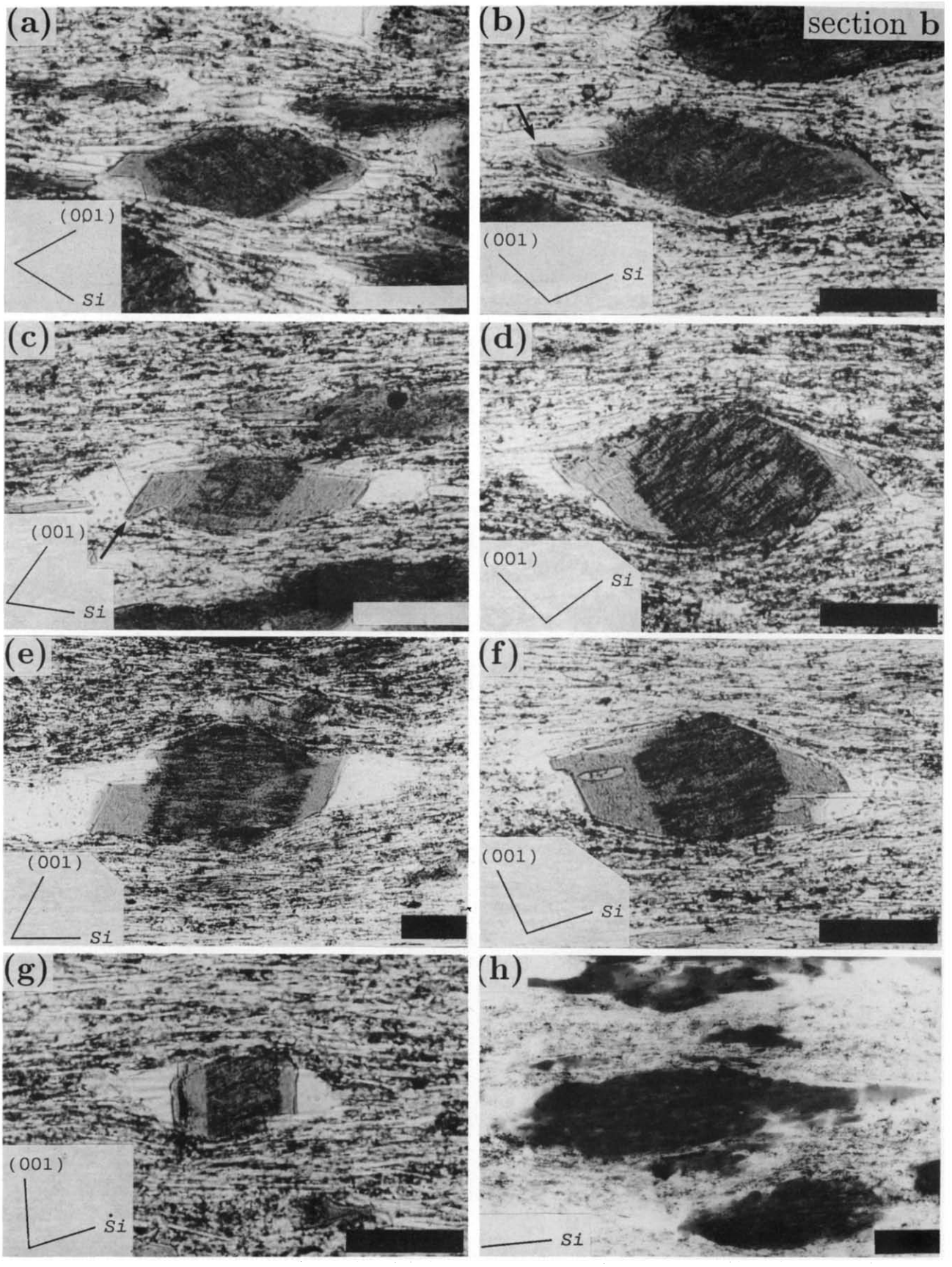


Fig. 5. 'Upright biotites' with various 'inclination angles' (a–g) and 'recumbent biotite' (h) in the **b**-section. In 'upright biotites' *Si* is sub-parallel to *Se* when (001) is inclined in anticlockwise direction by about 70° from *Se* (e). Biotites with clockwise inclination of *Si* are restricted to cases where (001) is inclined in anticlockwise direction by smaller angles (a & c). For details see Fig. 10(b). In 'recumbent biotite' (h), *Si* is sub-parallel to *Se*. Pressure shadows and inclusion free domains around 'upright biotites' in the **b**-section are better developed than those in the **a**-section. Arrows in (b) and (c) indicate hook-like tails of inclusion-free domains. Scale bars are 0.1 mm.

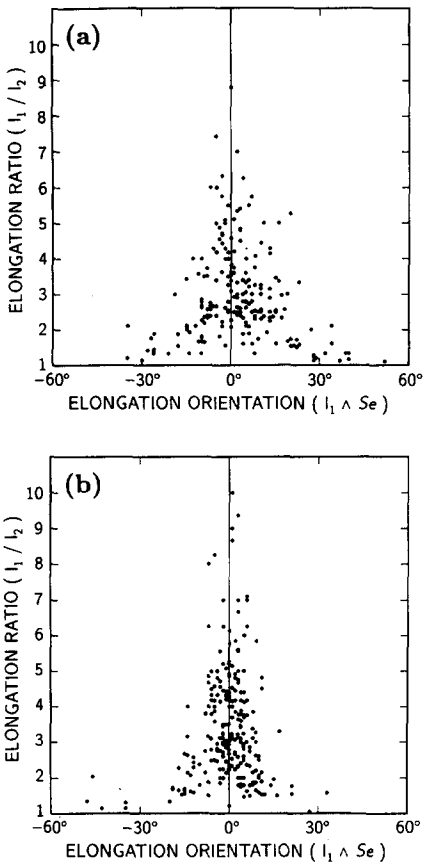


Fig. 6. Relationship between elongation orientation and elongation ratio of biotite grains in (a) the **a**-section and (b) the **b**-section.

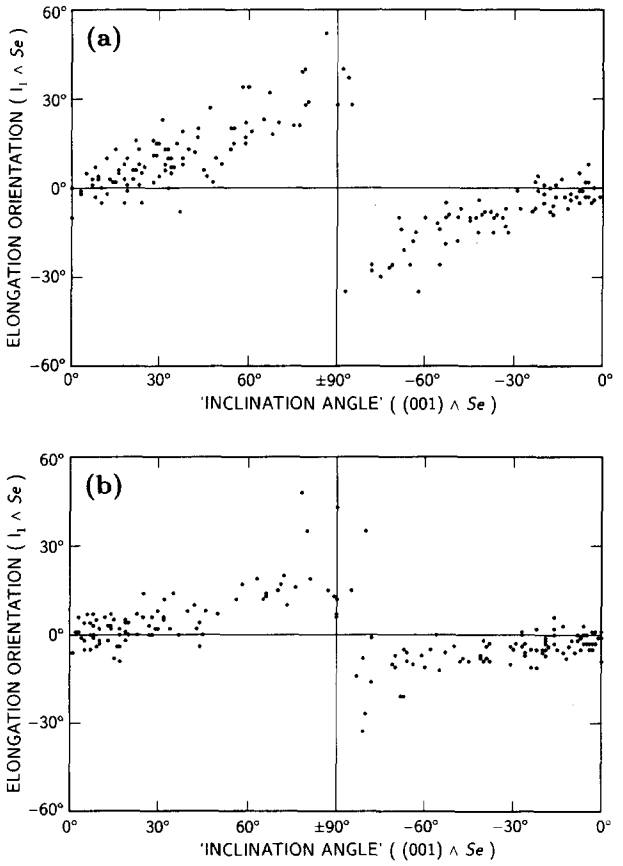


Fig. 7. Relationship between 'inclination angle' and elongation orientation of 'upright biotites' in (a) the **a**-section and (b) the **b**-section.

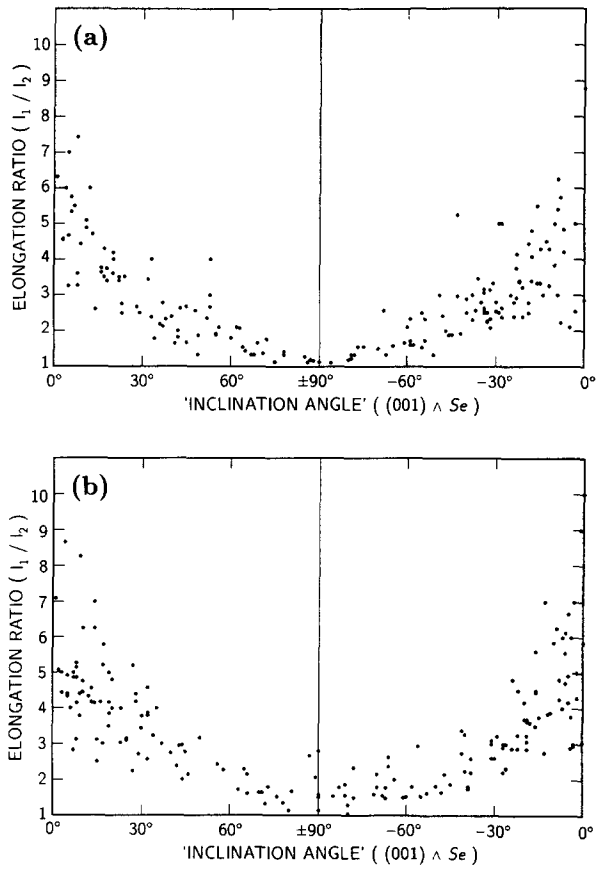


Fig. 8. Relationship between 'inclination angle' and elongation ratio of 'upright biotites' in (a) the **a**-section and (b) the **b**-section.

tation, it is possible that rotation of the biotite porphyroblasts occurred due to intracrystalline slip on (001) (cf. Mancktelow 1979). However intracrystalline deformation structures such as undulose extinction, kinking or waviness of the (001) cleavage are rare in the case of the present biotite porphyroblasts. In addition inclusion trails in the biotite porphyroblasts remain straight. These facts suggest that intracrystalline slip is not so significant. Biotite grains with many mineral inclusions could be more resistant to intracrystalline slip than inclusion-free grains, since intracrystalline deformation of included minerals would not be easy.

When intracrystalline slip on (001) is negligible, the discordant angle between *Si* and *Se* represents the rigid body rotation angle of the biotite grain. Figure 9 shows that there are two non-rotating orientations of 'upright biotite', respectively, in each of the **a**- and **b**-section planes. These non-rotating orientations include stable and unstable orientations (Passchier 1987) for rotations around the axes perpendicular to the section planes. The stable orientations have those of approximately 0° and 10° for **a**- and **b**-sections, respectively. On the other hand, the unstable orientations have 'inclination angles' of approximately 90° and 70° for **a**- and **b**-sections, respectively. Biotite grains are considered to have rotated towards the stable orientations, and biotite grains around the unstable orientations are thus expected to be scarce. The weak lattice fabric of biotite (Fig. 3) shows monoclinic symmetry and is consistent with the above stable and unstable orientations.

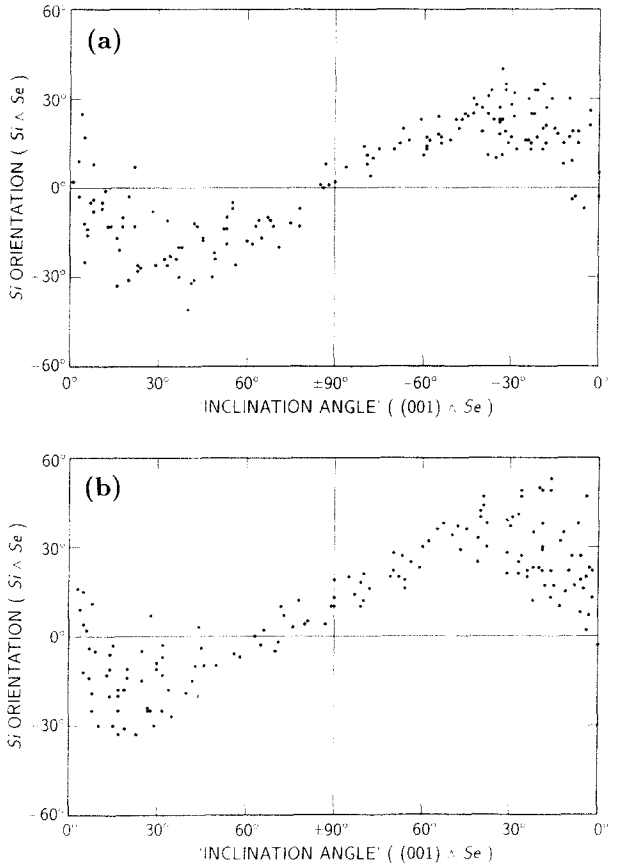


Fig. 9. Relationship between 'inclination angle' and *Si* orientation of 'upright biotites' in (a) the **a**-section and (b) the **b**-section. Note that the variation trend is symmetrical with respect to the *Se* trace in (a) but is asymmetric in (b).

The presence of the hook-like tails of inclusion-free domains (Figs. 4d & e and 5b & c) suggests that rotation and shape change of biotite porphyroblasts occurred simultaneously. The formation of the tail can be interpreted in the following way. When an (001) face lies in the extension field, some porphyroblast corners will rotate towards the center of the pressure shadow forming part. In response to dilation within the pressure shadow, the (001) face will be advanced by new biotite growth in the direction normal to the face. At the same time, new biotite growth will also occur at the same porphyroblast corners in a direction parallel to (001), since the volume dilated at the corners must be filled during progressive rotation. On the other hand, the opposite porphyroblast corners which rotate towards the shortening field will be dissolved. Thus the characteristic hook-like tail and the asymmetric shape of the inclusion-free domain can be formed by growth during progressive rotation of the biotite grains.

The systematic variation of the *Si* orientation can be explained in terms of rigid body rotation of biotite grain. As a first approximation, it will be assumed that the matrix is a homogeneous material and behaves like a viscous fluid during ductile deformation. In this case non-equidimensional rigid porphyroblasts should rotate at different rates around the different axes according to their shape and shape orientation with respect to the strain field (Passchier 1987).

Direct information about the initial shape of the biotite porphyroblasts has been lost as a result of the solution mass removal of biotite. However, it can be assumed that the initial porphyroblasts were platy and elongate along the (001) plane on the basis of the two-dimensional shape of the inclusion-crowded domain of 'upright biotite' in the **c**-section (Figs. 4g & h). The systematic variation patterns of *Si* in **a**- and **b**-sections can be developed under a mildly non-coaxial deformation, which includes a pure shear flattening perpendicular to the schistosity and a simple shearing sub-parallel to the schistosity in a direction sub-parallel to the lineation. The above setting of the deformation components suggests that the extensional eigenvector plane (Passchier 1986) was nearly parallel to the schistosity.

When 'upright biotites' in the **a**-section are considered, only a pure shear component contributes to the porphyroblast rotation around the axis perpendicular to the section plane since the shearing direction in the simple shear component is perpendicular to the section plane. In this case porphyroblasts will rotate such that the elongation direction approaches the schistosity, so that the porphyroblasts inclined in clockwise and anticlockwise directions from the schistosity will rotate in the anticlockwise and clockwise directions, respectively, and the non-rotating (001) orientations lie at positions perpendicular and parallel to the schistosity trace (Fig. 10a). This leads to the symmetric variation pattern for the **a**-section as seen in Fig. 9(a).

On the other hand, rotation of 'upright biotite' porphyroblasts in the **b**-section will be affected by both pure and simple shear components. In this case, the simple shearing component tends to rotate the porphyroblast all in the same direction, while the contribution of the pure shear component is similar to the case for the **a**-section. If the simple shear component is small enough relative to the axial ratio of biotite grains, two non-rotating (001) orientations will still exist (Ghosh & Ramberg 1976, Passchier 1987). However, the non-rotating orientations will depart from the positions normal and parallel to the schistosity trace (Fig. 10b). This leads to the asymmetric rotation pattern observed for the **b**-section in Fig. 9(b).

In the above discussion, rotation of biotite porphyroblasts was interpreted under the assumption that the biotite grains behaved like rigid particles embedded in a homogeneous matrix which deformed like a viscous fluid. However, since (1) shape change and (2) fracturing along the (001) face and deposition of pressure shadow aggregates have occurred concurrently with rotation, it is clear that this assumption is not completely valid. Therefore, some modifications may be needed to the present interpretation. Combination of shape change and rigid body rotation of biotite grains will accelerate rotation of their elongation orientation. As a result, the elongation orientation of a biotite porphyroblast could approach the stable position by a smaller

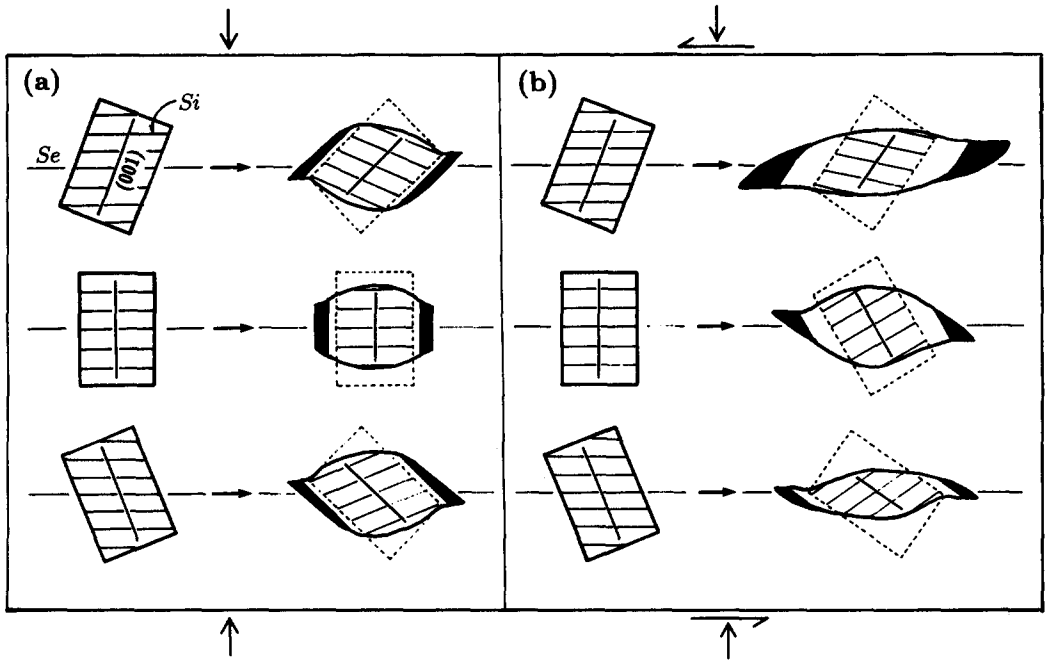


Fig. 10. Schematic illustration showing shape change and rotation of 'upright biotites' with different 'inclination angles' in (a) the a-section and (b) the b-section. In the a-section (a), only a pure shear component of deformation is important for shape change and rotation, while in the b-section (b), both pure and simple shear components are important. Pressure shadows in grey.

amount of rigid body rotation compared to the case of no shape change.

## DISCUSSION AND CONCLUSIONS

Since publication of Bell & Rubenach (1983) some researchers have claimed that rigid porphyroblasts do not generally rotate even during non-coaxial progressive deformation and have explained the lack of porphyroblast rotation in terms of deformation partitioning into coaxial and non-coaxial zones (Bell 1985, 1986, Bell *et al.* 1986, 1992, Bell & Johnson 1989, Steinhardt 1989, Johnson 1990, Hayward 1990, 1992). Especially Bell (1985) argued that porphyroblasts that do not deform generally cause strong deformation partitioning around the porphyroblast, so that coaxially deforming ellipsoidal islands of porphyroblast width are produced, being protected from the effects of progressive shearing.

However, I feel that the deformation partitioning into coaxial and non-coaxial zones is not a cause but a result of non-rotation of porphyroblasts. In other words, if a porphyroblast does not rotate, such a deformation partitioning is possible, but if a porphyroblast rotates, another type deformation partitioning is expected around the porphyroblast. Ultimately, whether or not a porphyroblast rotates depends on whether or not the stress applied on the porphyroblast surface can produce an effective torque on the porphyroblast.

Here I will discuss the possibility of porphyroblast non-rotation in terms of the stress on the porphyroblast surface. Consider the simple situation where a rigid spherical porphyroblast is placed in a homogeneous matrix deforming non-coaxially. Due to the shearing couple sub-parallel to the shear plane of the simple shear component, the porphyroblast will rotate. At the same time, the rotation will cause a shearing couple of opposite direction on the surface at high angles to the shear plane, which will resist the rotation. The rotation rate is determined by the balance between these two kinds of shearing couples.

Regardless of the rotation rate, some deformation partitioning must occur around the rigid porphyroblast leading to a heterogeneous stress field in the matrix. Under such conditions, it is possible that mass transfer occurs among deformation-partitioned zones by a pressure solution mechanism (e.g. Rutter 1976). If mass transfer effectively occurs, a kind of compositional differentiation will be developed around the porphyroblast. A pressure shadow is a material representation of such compositional differentiation.

Once pressure shadows form on both sides of the porphyroblast, the porphyroblast rotation rate would be influenced by the viscosity contrast between the pressure shadows and the matrix. If the pressure shadow is viscous enough relative to the matrix, then the porphyroblast and the pressure shadows will possibly form a single elongate rotation unit (e.g. Johnson 1990). In this case, the rotation of the elongate unit will be very small at low angles to the shear plane (Passchier 1987).

In spite of the above discussion, microstructural observations strongly suggest that biotite porphyroblasts in the present sample did rotate. The key to understanding the rotation of these biotite porphyroblasts is the origin of the pressure shadows. In the above discussion, it was proposed that the higher viscosity of pressure shadows produced due to deformation partitioning tends to prevent porphyroblast rotation. However, the pressure

shadow aggregates in the present sample are considered to have originated from deposition in continuously opening microfractures at the (001) interfaces (cf. Ramsay 1980).

Generally, continuously opening fractures will cause a lowering of pressure in the opened space and filling by pore fluid migrating from the grain boundary network, accompanying with mass transfer of deposited materials. Thus the porphyroblast surface in contact with the fracture will be separated from solid pressure shadow aggregates by pore fluid. Therefore, the rotating system will be divided into three units: one porphyroblast itself and two pressure shadows, as Etchecopar & Malavieille (1987) assumed for one of the simulated models of pressure shadow development. In such an arrangement of the rotating system, porphyroblast rotation will be promoted since the force resisting rotation will be reduced, due to the reduction of the shear stress on the surface contact with the fracture. Therefore, porphyroblast rotation would be affected not by the higher viscosity of the pressure shadow aggregates but by the position of the fractures. Since fracturing of the biotite surface would preferentially occur along the (001) face, the rotation direction and rotation rate would depend not only on the shape and shape orientation but also immediately on the (001) face orientation.

From this discussion it can be concluded that 'deformation-partitioning-induced pressure shadow' and 'fracture-induced pressure shadow' formation play different roles in influencing porphyroblast rotation; the former suppresses porphyroblast rotation while the latter promotes it. The 'fracture-induced pressure shadow' may correspond to a 'pressure fringe' as defined by Spry (1969).

Vernon (1988) gave, as possible microstructural evidence for non-rotation of mica porphyroblasts, the presence of parallel inclusion trails in several nearby porphyroblasts. However, if the initial shape and orientation of nearby porphyroblasts are similar to each other, the parallel inclusion trails can also be explained in terms of rigid body rotation. The (001) faces of mica have a surface energy which is characteristically low. Therefore, fracturing along the (001) face should be relatively easy even during ductile deformation of the matrix. When mica porphyroblasts have 'fracture-induced pressure shadows', the discordance between *Si* and *Se* is considered to be caused mainly by rigid body rotation of the porphyroblast.

*Acknowledgements*—I thank C. W. Passchier and N. S. Mancktelow for suggesting numerous improvements to the manuscript. I also thank K. Suwa, K. Suzuki, H. Noro and T. Sawaki for constructive comments on an early version of this manuscript.

## REFERENCES

Asami, M. & Hoshino, M. 1980. Staurolite-bearing schists from the Hongu-san area in the Ryoke Metamorphic belt, central Japan. *J. geol. Soc. Jap.* **86**, 581–591.

Asami, M., Hoshino, M., Miyakawa, K. & Suwa, K. 1982. Metamorphic conditions of staurolite schists of the Ryoke metamorphic belt in the Hazu-Hongusan area, central Japan. *J. geol. Soc. Jap.* **88**, 437–450 (in Japanese with English abstract).

Bell, T. H. 1981. Foliation development—the contribution, geometry and significance of progressive, bulk, inhomogeneous shortening. *Tectonophysics* **75**, 273–296.

Bell, T. H. 1985. Deformation partitioning and porphyroblast rotation in metamorphic rocks: a radical reinterpretation. *J. metamorph. Geol.* **3**, 109–118.

Bell, T. H. 1986. Foliation development and refraction in metamorphic rocks: reactivation of earlier foliations and decrenulation due to shifting patterns of deformation partitioning. *J. metamorph. Geol.* **4**, 421–444.

Bell, T. H., Fleming, P. D. & Rubenach, M. J. 1986. Porphyroblast nucleation, growth and dissolution in regional metamorphic rocks as a function of deformation partitioning during foliation development. *J. metamorph. Geol.* **4**, 37–67.

Bell, T. H. & Johnson, S. E. 1989. Porphyroblast inclusion trails: the key to orogenesis. *J. metamorph. Geol.* **7**, 279–310.

Bell, T. H. Johnson, S. E., Davis, B., Forde, A., Hayward, N. & Wilkins, C. 1992. Porphyroblast inclusion-trail orientation data: *eppure non son girate! J. metamorph. Geol.* **10**, 295–307.

Bell, T. H. & Rubenach, M. J. 1983, Sequential porphyroblast growth and crenulation cleavage development during progressive deformation. *Tectonophysics* **92**, 171–194.

Beutner, E. C. 1978. Slaty cleavage and related strain in Martinsburg slate, Delaware Water Gap, New Jersey. *Am. J. Sci.* **278**, 1–23.

Carter, N. L. 1976. Steady state flow of rocks. *Rev. Geophys. & Space Phys.* **14**, 301–360.

Cox, F. C. 1969. Inclusions in garnets: discussion and suggested mechanisms of growth for syntectonic garnets. *Geol. Mag.* **106**, 57–62.

Etchecopar, A. 1977. A plane kinematic model of progressive deformation in a polycrystalline aggregate. *Tectonophysics* **39**, 121–139.

Etchecopar, A. & Malavieille, J. 1987. Computer models of pressure shadows: a method for strain measurement and shear-sense determination. *J. Struct. Geol.* **9**, 667–677.

Ferguson, C. C. 1979. Rotation of elongate rigid particles in slow non-Newtonian flows. *Tectonophysics* **60**, 247–262.

Fyson, W. K. 1975. Fabrics and deformation of Archean metasedimentary rocks, Ross Lake–Gordon Lake area, Slave Province, Northwest Territories. *Can J. Earth Sci.* **12**, 765–776.

Fyson, W. K. 1980. Fold fabrics and emplacement of an Archean granitoid pluton, Cleft Lake, Northwest Territories. *Can. J. Earth Sci.* **17**, 325–332.

Gay, N. G. 1968. Pure shear and simple shear deformation of inhomogeneous viscous fluids. 1, Theory. *Tectonophysics* **5**, 211–234.

Ghosh, S. & Ramberg, H. 1976. Reorientation of inclusions by combination of pure shear and simple shear. *Tectonophysics* **34**, 1–70.

Hayward, N. 1990. Determination of early fold axis orientations in multiply deformed rocks using porphyroblast inclusion trails. *Tectonophysics* **179**, 353–369.

Hayward, N. 1992. Microstructural analysis of the classical spiral garnet porphyroblasts of south-east Vermont: evidence for non-rotation. *J. metamorph. Geol.* **10**, 567–587.

Jeffery, G. B. 1922. The motion of ellipsoidal particles immersed in a viscous fluid. *Proc. R. Soc. Lond.* **A102**, 161–179.

Johnson, S. E. 1990. Lack of porphyroblast rotation in the Otago schists, New Zealand: implications for crenulation cleavage development, folding and deformation partitioning. *J. metamorph. Geol.* **8**, 13–30.

Kano, K. 1978. Stratigraphy and structure of the Ryoke metamorphic rocks in Aichi Prefecture, Central Japan. *J. geol. Soc. Jap.* **84**, 445–458 (in Japanese with English abstract).

Lister, G. S., Boland, J. N. & Zwart, H. J. 1986. Step-wise growth of biotite porphyroblasts in pelitic schists of the western Lys-Caillaouas massif (Pyrenees). *J. Struct. Geol.* **8**, 543–562.

Lister, G. S. & Williams, P. F. 1983. The partitioning of deformation in flowing rock masses. *Tectonophysics* **92**, 1–33.

Mancktelow, N. S. 1979. The development of slaty cleavage, Fleurieu Peninsula, south Australia. *Tectonophysics* **58**, 1–20.

Nozawa, T. 1977. Radiometric age map of Japan. Scale 1:2,000,000. Geological Survey of Japan, Tokyo.

Olesen, N. O. 1982. Heterogeneous strain of a phyllite as revealed by porphyroblast–matrix relationship. *J. Struct. Geol.* **4**, 481–490.

Passchier, C. W. 1986. Flow in natural shear zones—the consequences of spinning flow regimes. *Earth Planet Sci. Lett.* **77**, 70–80.

Passchier, C. W. 1987. Stable positions of rigid objects in non-coaxial flow—a study in vorticity analysis. *J. Struct. Geol.* **9**, 679–690.

Passchier, C. W., Trouw, R. A. J., Zwart, H. J. & Vissers, R. L. M. 1992. Porphyroblast rotation: eppur si muove? *J. metamorph. Geol.* **10**, 283–294.

Powell, D. & Treagus, J. E. 1970. Rotational fabrics in metamorphic minerals. *Mineralog. Mag.* **37**, 801–814.

Ramsay, J. G. 1962. The geometry and mechanics of formation of 'Similar' type folds. *J. Geol.* **70**, 309–327.

Ramsay, J. G. 1980. The crack-seal mechanism of rock deformation. *Nature* **282**, 135–139.

Rast, N. 1965. Nucleation and growth of metamorphic minerals. In: *Controls of Metamorphism* (edited by Pitcher, W. S. & Flinn, C. W.), 73–102.

Rutter, E. H. 1976. The kinetics of rock deformation by pressure solution. *Phil. Trans. R. Soc. Lond.* **A283**, 203–219.

Seo, T. 1985. The study of the Ryoke metamorphism in view of metamorphic history and conditions: as illustrated in the metamorphic terrain of the southwestern part of Mikawa Plateau. *Geol. Hiroshima Univ.* **27**, 93–155 (in Japanese with English abstract).

Seo, T. & Hara, I. 1980. The development of schistosity in biotite schists from southwestern part of Mikawa Plateau, central Japan. *J. geol. Soc. Jap.* **86**, 817–826.

Spry, A. 1963. Origin and significance of snowball structure in garnet. *J. Petrol.* **4**, 211–222.

Spry, A. 1969. *Metamorphic Textures*. Pergamon Press, Oxford.

Steinhardt, C. K. 1989. Lack of porphyroblast rotation in non-coaxially deformed schists from Petrel-Cove, South Australia, and its implications. *Tectonophysics* **158**, 127–140.

Vernon, R. H. 1988. Microstructural evidence of rotation and non-rotation of mica porphyroblasts. *J. metamorph. Geol.* **6**, 255–270.

Williams, P. F. & Schoneveld, C. 1981. Garnet rotational and the development of axial plane crenulation cleavage. *Tectonophysics* **78**, 307–334.

Zwart, H. J. 1962. On the determination of polymetamorphic mineral associations, and its application to the Bosost area (Central Pyrenees). *Geol. Rdsch.* **52**, 38–65.

Zwart, H. J. & Calon, T. J. 1977. Chloritoid crystals from Curaglia; growth during flattening or pushing aside? *Tectonophysics* **39**, 477–486.